Impact of P-Glycoprotein on Blood–Retinal Barrier Permeability: Comparison of Blood–Aqueous Humor and Blood–Brain Barrier Using *Mdr1a* Knockout Rats

Shinobu Fujii,[1,2] Chikako Setoguchi,[1] Kouichi Kawazu,[1] and Ken-ichi Hosoya[2]

[1]Nara Research and Development Center, Santen Pharmaceutical Co., Ltd., Nara, Japan
[2]Department of Pharmaceutics, Graduate School of Medicine and Pharmaceutical Sciences, University of Toyama, Toyama, Japan

Correspondence: Shinobu Fujii, Nara Research and Development Center, Santen Pharmaceutical Co., Ltd., 8916-16 Takayama-cho, Ikoma-shi, Nara 630-0101, Japan; shinobu.fujii@santen.co.jp.

Submitted: December 22, 2013
Accepted: June 17, 2014

Citation: Fujii S, Setoguchi C, Kawazu K, Hosoya K. Impact of P-glycoprotein on blood–retinal barrier permeability: comparison of blood–aqueous humor and blood–brain barrier using *mdr1a* knockout rats. *Invest Ophthalmol Vis Sci*. 2014;55:4650–4658. DOI:10.1167/iovs.13-13819

Purpose. The purpose of this study was to clarify the impact of P-glycoprotein (P-gp) on blood–retinal barrier (BRB) and blood–aqueous humor barrier (BAB) permeability, in contrast to blood–brain barrier (BBB) permeability.

Methods. Permeabilities of six compounds, including P-gp substrates (quinidine, digoxin, and verapamil), were investigated in wild-type and *mdr1a* knockout rats using retinal, aqueous humor, and brain uptake index (RUI, AHUI, and BUI, respectively) methods and integration plot analysis.

Results. In both rat strains, quinidine, digoxin, and verapamil were transported by P-gp across each barrier; however, the impact of P-gp on retinal uptake of quinidine and verapamil was less pronounced than that on brain uptake. The apparent influx permeability clearance (K_{in}) values of verapamil in retina obtained from wild-type and knockout rats were similar (0.824 ± 0.201 and 0.849 ± 0.980 mL/min·g retina, respectively; mean ± SD; $n = 3$ rats). The K_{in} in aqueous humor and brain obtained from knockout rats was, respectively, 3-fold and 12-fold higher than that of wild-type ($P < 0.05$). In P-gp–deficient conditions, the RUI and AHUI of quinidine, digoxin, and verapamil, as well as the BUI of quinidine and digoxin, were decreased by P-gp inhibitors. However, the BUI of verapamil was not changed by P-gp inhibitors. Results suggest that carrier-mediated influx transporters exist in the blood–ocular barriers and that the function of verapamil influx transporters is markedly different between the retina and brain.

Conclusions. In both rat strains, P-gp operates in the blood–ocular barriers, and the impact of P-gp on BRB permeability to quinidine and verapamil is lower than that on BBB permeability.

Keywords: P-glycoprotein, blood–retinal barrier, *mdr1a* knockout rat, blood–ocular barrier

Many ocular diseases involve pathologic conditions of the retina. Age-related macular degeneration is a progressive retinal degenerative disease caused by extensive choriocapillaris loss, death of the RPE, and/or choroidal neovascularization, leading to severe central vision loss in the elderly population.[1] Retinal neovascularization and the resulting vascular hyperpermeability cause vision loss in diabetic retinopathy.[2] Retinitis pigmentosa involves disturbances in retinal metabolism, pigment clumping at the RPE, and manifests as progressive visual field loss, night blindness, and abnormal electroretinography.[3]

Chronic retinal disorders such as these typically are treated by periocular or intraocular drug injections or implantations,[4] but these routes of administration are invasive and pose safety risks to patients, including infection, retinal detachment, and vitreous hemorrhage. Systemic drug administration is a possible alternative for treating retinal diseases. However, penetration of drugs from circulating blood to the posterior segment of the eye is strictly regulated by blood–ocular barriers, namely, the blood–aqueous humor barrier (BAB) and the blood–retinal barrier (BRB),[5,6] just as the brain is protected strictly by the blood–brain barrier (BBB).

The BAB is formed by two discrete layers of cells, the endothelium of the blood vessels of the iris and the nonpigmented layer of the ciliary epithelium. Tight junctional complexes are present in both cell layers.[7] Similarly, the BRB consists of retinal capillary endothelial cells (inner BRB) and the RPE cells (outer BRB),[6] and is created by the complex tight junctions of both cells. The BAB and BRB have a role in the influx transport of essential molecules and the efflux transport of endobiotics and xenobiotics, to control the intraocular environment and maintain neuroretinal homeostasis. Interestingly, ATP-binding cassette (ABC) and solute carrier (SLC) drug transporters are reported to be expressed at the blood–ocular barriers,[8] similar to the BBB.[9]

One of the ABC transporters, P-glycoprotein (P-gp, also known as Mdr1 and Abcb1), is expressed in iris, ciliary muscle, and ciliary nonpigmented cells,[10–12] which are part of the BAB. Various SLC transporters, organic cation/carnitine transporter (OCTN) 1 (SLC22A4), OCTN2 (SLC22A5), organic cation transporter 1 (OCT1; SLC22A1), and organic anion transporter 3 (OAT3; SLC22A8) are expressed in the human iris-ciliary body,[12] and organic anion transporting polypeptides1a4 (oatp2; slco1a4), 1a5 (oatp3; slco1a5), and 1b2 (oatp4; slco1b2) are found in the rat ciliary body.[13] Furthermore, in the BRB, P-gp is

localized in the luminal membrane of retinal capillary endothelial cells,[5,14,15] and in the apical and basal sides of the RPE.[15] The expression of SLC transporters, such as OCTNs, oatp families, and novel cationic transporters, also has been reported in the inner and/or outer BRB.[8] According to these reports,[14,15] the contribution of P-gp in the inner BRB is lower than that in the BBB; accordingly, Toda et al.[16] and Hosoya et al.[17] have reported that in rats, the P-gp function is less active in the BRB than in the BBB. In the rat genome, there are two paralogous genes encoding P-gp, *mdr1a* and *mdr1b*. Among most of the P-gp substrates that we tested in this study, including quinidine, digoxin, and verapamil, there were no differences between rat *mdr1a* and *mdr1b* in P-gp substrate recognition.[18] However, *mdr1a* is the predominant form in the rat inner BRB[19] as well as the BBB,[20] although the predominant form in rat outer BRB and BAB still is unclear.

As is well known, transporters may represent rate-limiting steps in drug absorption, distribution, and elimination in the small intestine, liver, kidney, and BBB. As mentioned above, the blood–ocular barriers are expected to be physiologically similar to the BBB, but the precise details still are unknown. This is because the complex structures of the BAB and BRB are composed of two cell types, which makes clarifying the mechanisms of carrier-mediated drug transport in in vivo studies problematic. Moreover, P-gp has a broad range of substrate specificity, meaning that many drugs are recognized by P-gp as well as by other influx/efflux transporters. Therefore, the *mdr1a* knockout rat model[21,22] is a powerful in vivo tool to elucidate the impact of P-gp on the retinal distribution of drugs and to reveal the function of carrier-mediated drug transporters in the BAB and BRB under P-gp–deficient conditions. It has been reported that in this model, *mdr1a* expression is reduced 8- to 23-fold in the brain, intestine, liver, and kidney, but *mdr1b* expression is not upregulated.[22]

This study aimed to clarify the function and impact of P-gp on BRB, BAB, and BBB permeability using *mdr1a* knockout rats. The characteristics of quinidine, digoxin, and verapamil transport and inhibition across the BRB and BAB, compared to the BBB, also were investigated using *mdr1a* knockout rats lacking functional P-gp. Our results provided valuable information on predicting drug penetration across the blood–ocular barriers as well as designing optimal drug candidates or drug delivery systems for treating ocular diseases.

Materials and Methods

Animals

Male wild-type Sprague-Dawley rats (6–8 weeks) were obtained from Charles River Laboratories Japan, Inc. (Yokohama, Japan). Male Sprague-Dawley *mdr1a* knockout rats (7–10 weeks) were purchased from Sage Labs (St. Louis, MO, USA). Rats had free access to food and water. All experiments in this study involving animals complied with the Ethical Guidelines for Animal Experiments of Santen Pharmaceutical Company, Ltd. (Ikoma, Japan) and the ARVO Statement for the Use of Animals in Ophthalmic and Vision Research.

Reagents

Radiolabeled D-[1-^{14}C]mannitol ([^{14}C]D-mannitol, 55 mCi/mmol), [1,2,6,7-^{3}H]progesterone ([^{3}H]progesterone, 0.1 mCi/mmol), [p-^{3}H]quinidine ([^{3}H]quinidine, 0.02 mCi/mmol), [*N*-methyl-^{3}H]verapamil hydrochloride ([^{3}H]verapamil, 0.08 mCi/mmol), and *n*-[1-^{14}C]butanol ([^{14}C]*n*-butanol, 2 mCi/mmol) were purchased from American Radiolabeled Chemicals, Inc. (St. Louis, MO, USA). [^{3}H(G)]Digoxin ([^{3}H]digoxin, 29.8 Ci/mmol) was purchased from PerkinElmer Life and Analytical Sciences (Waltham, MA, USA). [^{14}C]Thiourea (59.4 mCi/mmol) and [^{3}H]water (25 mCi/mL) were purchased from Moravek Biochemicals, Inc. (Brea, CA, USA). All other chemicals were of reagent grade and were readily available from commercial sources.

Uptake Index Method

The retinal uptake index (RUI), aqueous humor uptake index (AHUI), and brain uptake index (BUI) were determined using previously reported uptake index methods.[16,23] Briefly, the *mdr1a* knockout and wild-type rats (n = 3–6/group) were anesthetized with an intramuscular injection of 125 mg/kg ketamine and 1.22 mg/kg xylazine. A 0.2-mL Ringer-HEPES buffer (141 mM NaCl, 4 mM KCl, 2.8 mM $CaCl_2$, and 10 mM HEPES; pH 7.4) containing [^{3}H]-labeled substances (10 μCi/rat) with [^{14}C]*n*-butanol (0.1 μCi/rat) as the highly diffusible reference or containing [^{14}C]-labeled substances (1 μCi/rat) with [^{3}H]water (5 μCi/rat) as the highly diffusible reference was injected into the carotid artery. To evaluate the effect of transporter inhibition, each inhibitor was administered simultaneously with test substances. Rats were decapitated 15 seconds after injection and the aqueous humor, retina, and cerebrum were removed and dissolved in a toluene-based tissue solubilizer (Soluen-350; PerkinElmer Life and Analytical Sciences). Radioactivity in tissues was measured using a liquid scintillation counter (TRI-CARB 2100TR; PerkinElmer Life and Analytical Sciences), and the RUI, AHUI, and BUI values were calculated according to Equations 1 and 2:

[^{3}H]-labeled substances (highly diffusible reference substance, [^{14}C]*n*-butanol):

$$\text{Uptake index}(UI,\%) = \left(\left[^{3}\text{H}\right]/\left[^{14}\text{C}\right]\text{dpm in the tissue}\right) / \left(\left[^{3}\text{H}\right]/\left[^{14}\text{C}\right]\text{dpm in the injectate}\right) \times 100 \quad (1)$$

[^{14}C]-labeled substances (highly diffusible reference substance, [^{3}H]water):

$$\text{Uptake index}(UI,\%) = \left(\left[^{14}\text{C}\right]/\left[^{3}\text{H}\right]\text{dpm in the tissue}\right) / \left(\left[^{14}\text{C}\right]/\left[^{3}\text{H}\right]\text{dpm in the injectate}\right) \times 100. \quad (2)$$

Integration Plot Analysis

Integration plot analysis was performed as described previously.[24] Briefly, [^{3}H]verapamil (10 μCi/rat) in 0.4 mL extracellular fluid buffer (122 mM NaCl, 25 mM $NaHCO_3$, 3 mM KCl, 1.4 mM $CaCl_2$, 1.2 mM $MgSO_4$, 0.4 mM K_2HPO_4, 10 mM D-glucose, and 10 mM HEPES; pH 7.4) with 100 IU/mL heparin was injected into the femoral vein of rats anesthetized with 125 mg/kg ketamine and 1.22 mg/kg xylazine. At 0.5, 1, 2, 3, and 5 minutes after injection, blood was collected and all rats were decapitated, after which the aqueous humor, retina, and cerebrum were removed. Collected tissues and plasma, prepared by centrifugation (approximately 1500*g*) of the blood sample, were dissolved in tissue solubilizer and radioactivity in the tissues was measured by liquid scintillation counting. The apparent influx permeability clearance (K_{in}) of [^{3}H]verapamil in the tissues was determined by Equation 3 and compared between *mdr1a* knockout rats and wild-type rats (n = 3/time point).

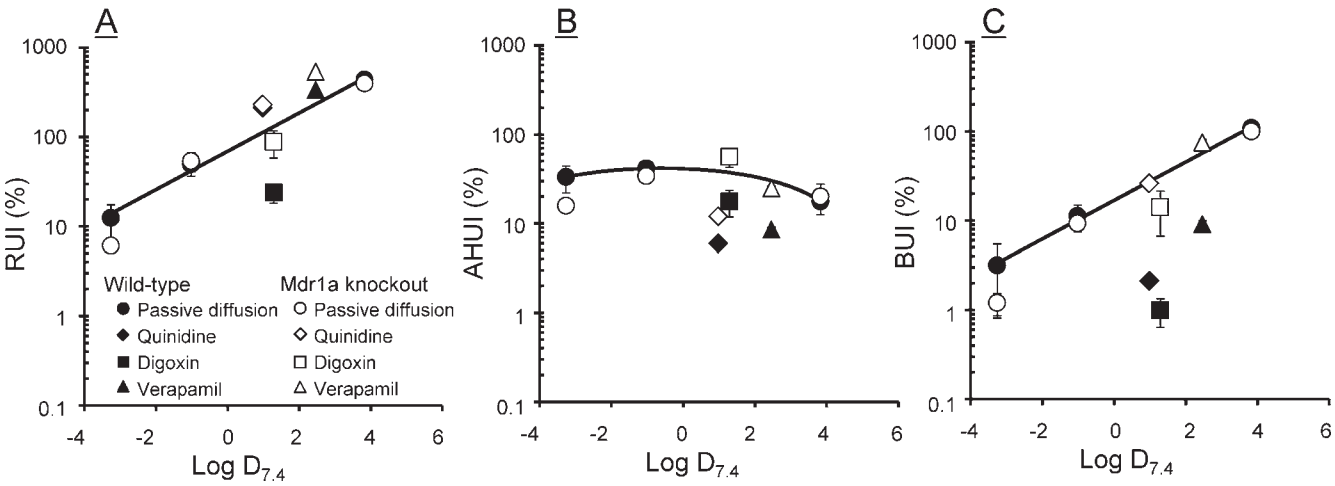

Figure 1. Correlation of the RUI (**A**), AHUI (**B**), and BUI (**C**) with Log $D_{7.4}$ for tested compounds (Table 1) in wild-type (*closed symbols*) and *mdr1a* knockout (*open symbols*) rats. The log $D_{7.4}$ value of each compound was calculated using Log D version 12.0 (Advanced Chemistry Development, Inc., Toronto, Ontario, Canada). The *line* represents the lipophilicity trend line in wild-type rats using the data of D-mannitol, thiourea, and progesterone, which are expected to permeate by passive diffusion. The *line* represents the linear regression curve (**A**, **C**) or the quadric regression curve (**B**) by the linear least-squares methods for the three compounds (passive diffusion, Table 1) in wild-type rats. RUI = 69.4 × exp (0.493 × Log $D_{7.4}$) ($r^2 = 0.993$) (**A**), AHUI = 1.22 × (Log $D_{7.4}$)^2 − 1.48 × Log $D_{7.4}$ + 41.2 ($r^2 = 1.00$) (**B**), and BUI = 16.9 × exp (0.496 × Log $D_{7.4}$) · ($r^2 = 0.998$) (**C**). *Points* represent means ± SE (n = 3–6 rats).

$$C_{app}(t)/C_p(t) = K_{in,tissue} \times AUC(t)/C_p(t) + V_i \qquad (3)$$

Here, $C_{app}(t)$(dpm/g tissue), $C_p(t)$(dpm/mL), AUC(t) ·(dpm·min/mL), and V_i(mL/g tissue) are the apparent tissue [^{3}H]verapamil concentration at time t, the plasma [^{3}H]verapamil concentration at time t, the area under the plasma concentration time curve of [^{3}H]verapamil from time 0 to t, and the rapidly equilibrated distribution volume of [^{3}H]verapamil in the tissue, respectively. V_i usually is comparable with the extracellular space.

Data Analysis

All data are expressed as means ± SE except for kinetic parameters, which are expressed as means ± SD. The unpaired, 2-tailed Student's t-test was used to assess the significance of the differences between the means of the two groups. Statistical significance of differences among means of several groups was determined by Bartlett's test followed by Dunnett's multiple comparison test. Statistical significance was set at $P < 0.05$.

Results

Comparison of RUI, AHUI, and BUI in Wild-Type and *mdr1a* Knockout Rats

To determine the effects of lipophilicity on drug permeability across the BRB, BAB, and BBB of *mdr1a* knockout rats, we assessed the RUI, AHUI, and BUI of three compounds that were expected to permeate by passive diffusion across a biological membrane with Log $D_{7.4}$ values ranging from −3.26 to 3.83 (Fig. 1; Table 1). The RUI, AHUI, and BUI values of the three compounds permeated in this manner were similar in wild-type and *mdr1a* knockout rats. Following the increase in Log $D_{7.4}$, the RUI and BUI values increased; in contrast, the AHUI values remained relatively unchanged.

Table 1. Classification and Log $D_{7.4}$ of the Tested Compounds

Classification	Compounds	Log $D_{7.4}$*
Passive diffusion	D-mannitol	−3.26
	Thiourea	−1.02
	Progesterone	3.83
Active transport	Quinidine	0.98
	Digoxin	1.29
	Verapamil	2.46

* The log $D_{7.4}$ value of each compound was calculated using Log D version 12.0 (Advanced Chemistry Development, Inc.).

Based on the results of quantitative real-time RT-PCR using freshly isolated rat RPE cells, the transcript level of *mdr1a* was 190-fold higher than that of *mdr1b* (see Supplementary Methods, Supplementary Fig. S1), as in the inner BRB[19] and BBB.[20] To clarify the effect of P-gp on BRB, BAB, and BBB permeability, the RUI, AHUI, and BUI values of [^{3}H]quinidine, [^{3}H]digoxin, and [^{3}H]verapamil, which are known substrates of P-gp, were compared between the wild-type and *mdr1a* knockout rats (Fig. 1). All P-gp substrates tested in the wild-type rats had lower AHUI and BUI values than the values predicted from lipophilicity. However, [^{3}H]quinidine and [^{3}H]verapamil had higher RUI values than predicted from lipophilicity, except for [^{3}H]digoxin, which had a lower RUI value. In *mdr1a* knockout rats, the AHUI and BUI values of P-gp substrates, which were lower than the predicted values from the lipophilicity in wild-type rats, came close to the predicted levels. The RUI of [^{3}H]digoxin in *mdr1a* knockout rats increased to near the lipophilicity trend line. However, the RUI of [^{3}H]quinidine and [^{3}H]verapamil in *mdr1a* knockout rats was almost the same as that in wild-type rats. These results indicated that quinidine, digoxin, and verapamil are transported by P-gp across the BRB, BAB, and BBB, but the impact of P-gp on the uptake of quinidine and verapamil in the retina is lower than that in the brain.

Comparison of Influx Permeability Clearance in Wild-Type and *mdr1a* Knockout Rats

To investigate the in vivo blood-to-tissue influx permeability clearance of verapamil across the BRB, BAB, and BBB, integration plot analysis after intravenous injection of [^{3}H]verapamil to *mdr1a* knockout rats was performed and compared to wild-type rats (Fig. 2; Table 2). The $K_{in,retina}$ of [^{3}H]verap-

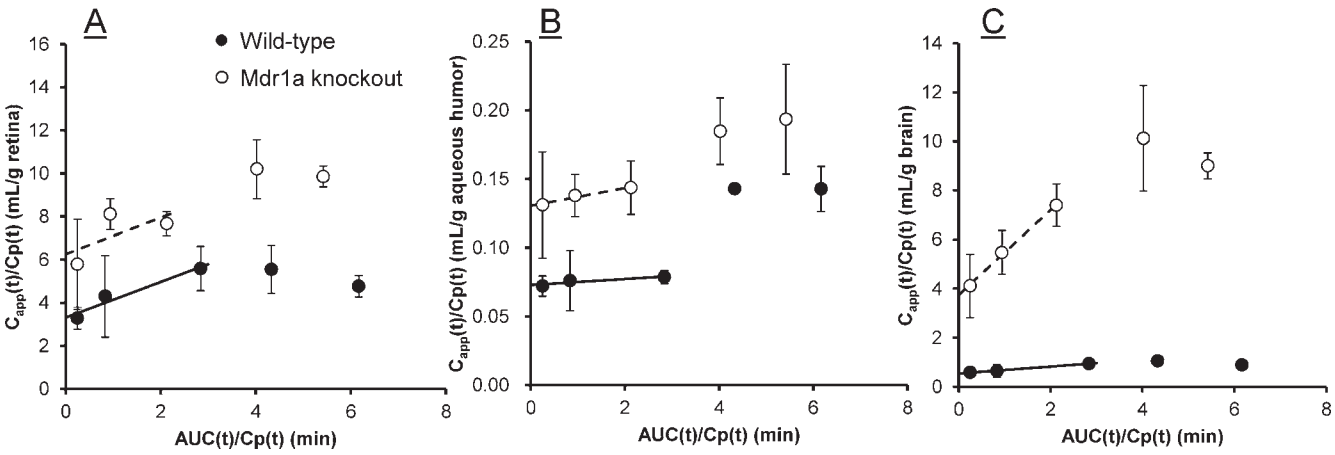

Figure 2. The initial uptake of [^{3}H]verapamil by the retina (**A**), aqueous humor (**B**), and brain (**C**) in wild-type (*closed circles*) and *mdr1a* knockout (*open circles*) rats. In the integration plot analysis, [^{3}H]verapamil was injected into the femoral vein. *Points* represent means ± SE ($n = 3$ rats). The *line* represents the regression line using the initial tissue uptake data in wild-type (*solid line*) and *mdr1a* knockout (*dashed line*) rats. The *slope* represents the apparent influx permeability clearance (K_{in}).

amil obtained from wild-type and *mdr1a* knockout rats was determined to be 0.824 ± 0.201 and 0.849 ± 0.980 mL/min·g retina (mean ± SD, $n = 3$ rats), respectively, which was not significantly different. The $K_{in,aqueousbumor}$ obtained from *mdr1a* knockout rats was 0.0065 ± 0.0013 mL/min·g aqueous humor (mean ± SD, $n = 3$ rats, $P < 0.05$), which was 3-fold higher than that obtained from wild-type rats. Also, $K_{in,brain}$ obtained from *mdr1a* knockout rats was 12-fold higher than that from wild-type rats ($P < 0.05$). The contribution of P-gp efflux of verapamil, measured in terms of the ratio of $K_{in,retina}$ between wild-type and *mdr1a* knockout rats, was 3.0%; in contrast, the contributions calculated from $K_{in,aqueousbumor}$ and $K_{in,brain}$ were 66.1% and 91.9%, respectively. These results clearly indicated that the impact of P-gp on BRB permeability to verapamil is lower than that on BAB and BBB permeability.

Inhibitory Effects of Several Compounds on [^{3}H]Quinidine, [^{3}H]Digoxin, and [^{3}H]Verapamil Influx

The effects of P-gp inhibitors on [^{3}H]quinidine, [^{3}H]digoxin, and [^{3}H]verapamil influx across the BRB, BAB, and BBB are summarized in Figure 3 and Table 3. In wild-type rats the RUI value of [^{3}H]quinidine did not significantly change with the addition of 10 mM quinidine and 3 mM verapamil; in contrast, significant increases were observed in the AHUI (2.0- and 2.4-fold higher than control, respectively; $n = 3$ rats/group; $P < 0.05$) and BUI values (8.6- and 6.2-fold higher than control, respectively; $n = 3$ rats/group; $P < 0.05$). Similarly, [^{3}H]verapamil influx across the BRB did not change with 1 mM vinblastine or 3 mM verapamil, although there were significant increases in the AHUI (1.8- and 2.7-fold, respectively; $n = 3$ rats/group; $P < 0.05$) and BUI values (4.7- and 8.6-fold, respectively; $n = 3$ rats/group; $P < 0.05$), compared to the absence of inhibitors. There was no change in [^{3}H]digoxin uptake in the retina, aqueous humor, or brain with P-gp inhibitors. These results in wild-type rats clearly showed that the P-gp–mediated efflux of [^{3}H]quinidine and [^{3}H]verapamil across the BAB and BBB is blocked by several inhibitors; in contrast, inhibitors have no significant effect on the BRB efflux, suggesting that the influence of P-gp on the uptake of quinidine and verapamil in the retina is lower than that in the brain.

With regard to *mdr1a* knockout rats, [^{3}H]quinidine influx in the retina nonsignificantly decreased with 10 mM quinidine by 19.5% compared to the control ($n = 3$ rats/group). Coadministration of [^{3}H]quinidine and 3 mM verapamil decreased the uptake of [^{3}H]quinidine in the retina, aqueous humor, and brain by 37.4%, 26.4%, and 52.6% of control, respectively ($n = 3$ rats/group; $P < 0.05$). Also, the RUI, AHUI, and BUI values of [^{3}H]digoxin with the addition of 0.01 mM digoxin and 3 mM verapamil were reduced by more than approximately 70% ($n = 3$ rats/group; $P < 0.05$). These results suggest that both compounds are permeated across the BRB, BAB, and BBB by carrier-mediated influx transporters. [^{3}H]Verapamil influx in the retina was decreased with 1 mM vinblastine and 3 mM verapamil by 32.4% and 29.3% of control, respectively ($n = 3$ or 5 rats/group, $P < 0.05$). In addition, the AHUI of [^{3}H]verapamil with 1 mM vinblastine was reduced by 46% of control ($n = 3$ rats/group, $P < 0.05$). However, the BUI value was unchanged by these inhibitors. While the results clearly indicated that [^{3}H]verapamil was permeated across the BRB and BAB by carrier-mediated influx transporters, there was no impact on the BBB by the influx transporters.

Table 2. The K_{in} per Gram of Rat Tissue of [^{3}H]Verapamil and the Contribution Ratio of P-gp to Tissue Uptake

	K_{in}, mL/min·g Tissue	V_i, mL/g Tissue	Contribution of P-gp, %
Wild-type			
Retina	0.824 ± 0.201	3.32 ± 0.34	3.0
Aqueous humor	0.0022 ± 0.0010	0.0728 ± 0.0017	66.1
Brain	0.140 ± 0.012	0.542 ± 0.020	91.9
Mdr1a knockout			
Retina	0.849 ± 0.980	6.25 ± 1.32*	–
Aqueous humor	0.0065 ± 0.0013*	0.130 ± 0.001*	–
Brain	1.73 ± 0.09*	3.75 ± 0.13*	–

The contribution of P-gp (%) is calculated from the following equation: $(K_{in,knockout} - K_{in,wild})/(K_{in,knockout}) \times 100$. Values represent means ± SD ($n = 3$ rats). V_i, the extracellular space.

* $P < 0.05$, significantly different from wild-type rat.

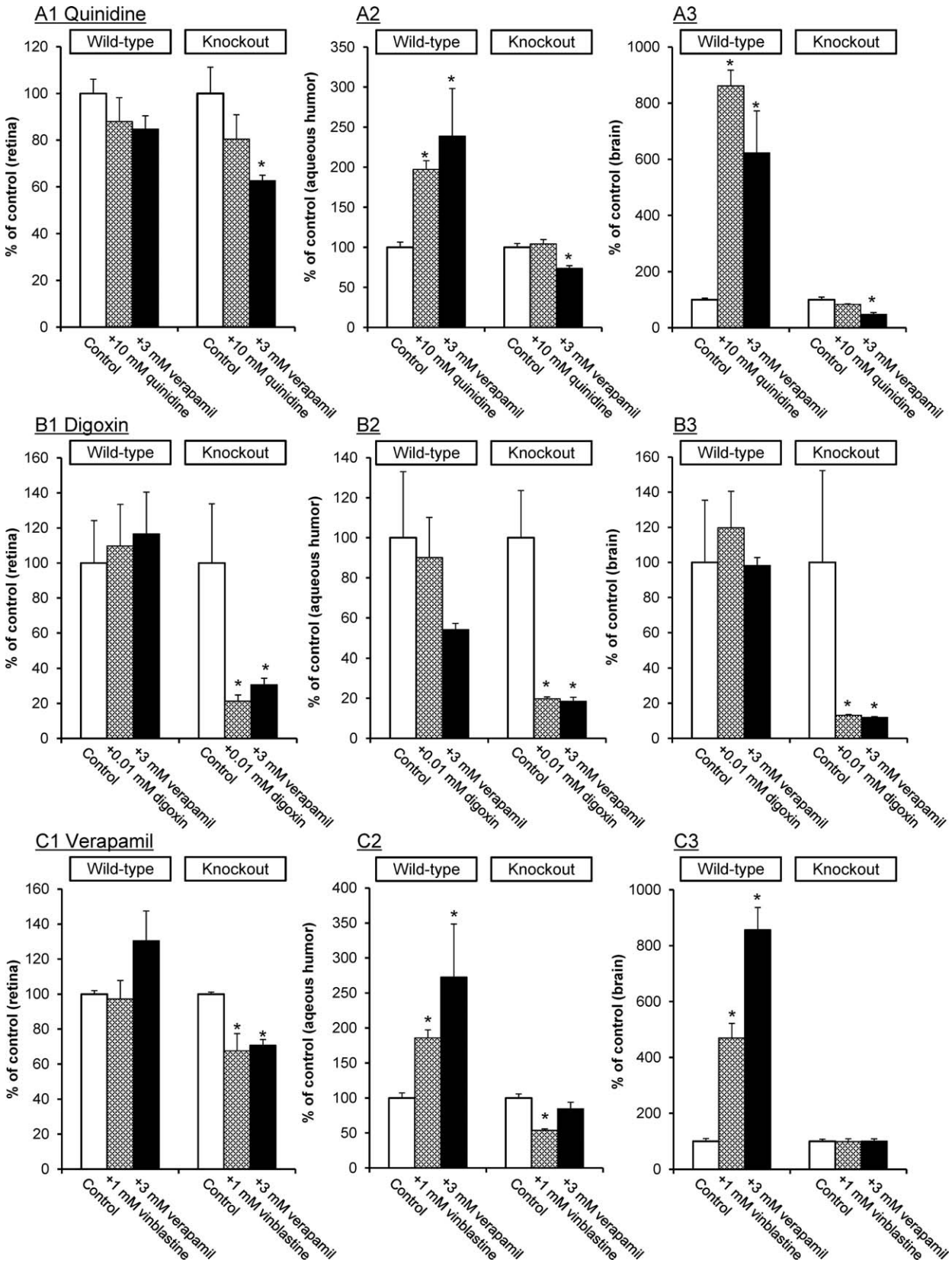

FIGURE 3. The effect of P-gp inhibitors on the RUI, AHUI, and BUI for [^{3}H]quinidine (**A1–A3**), [^{3}H]digoxin (**B1–B3**), and [^{3}H]verapamil (**C1–C3**) in wild-type and *mdr1a* knockout rats. Percent of control was calculated from data in Table 3. Values represent means + SE ($n = 3$–6 rats). *$P < 0.05$, significantly different from each control.

Table 3. The Effect of P-gp Inhibitors on the RUI, AHUI, and BUI for [^{3}H]Quinidine, [^{3}H]Digoxin, and [^{3}H]Verapamil in Wild-Type and *mdr1a* Knockout Rats

		Uptake Index, %		
	Inhibitor	**Retina**	**Aqueous Humor**	**Brain**
Wild-type				
Quinidine	Control	212 ± 13	5.95 ± 0.38	2.12 ± 0.12
	10 mM quinidine	187 ± 22	11.7 ± 0.6*	18.2 ± 1.2*
	3 mM verapamil	180 ± 12	14.2 ± 3.5*	13.2 ± 3.2*
Digoxin	Control	24.0 ± 5.8	17.5 ± 5.8	0.987 ± 0.350
	0.01 mM digoxin	26.3 ± 5.7	15.8 ± 3.5	1.18 ± 0.20
	3 mM verapamil	27.9 ± 5.7	9.48 ± 0.55	0.969 ± 0.045
Verapamil	Control	336 ± 7	8.46 ± 0.61	9.07 ± 0.89
	1 mM vinblastine	327 ± 35	15.7 ± 1.0*	42.5 ± 4.8*
	3 mM verapamil	439 ± 57	23.1 ± 6.4*	77.7 ± 7.2*
Mdr1a knockout				
Quinidine	Control	227 ± 25	12.0 ± 0.6†	26.1 ± 2.4†
	10 mM quinidine	182 ± 24	12.5 ± 0.7	21.6 ± 0.6
	3 mM verapamil	142 ± 5*	8.83 ± 0.40*	12.4 ± 1.7*
Digoxin	Control	88.0 ± 29.7†	55.9 ± 13.2†	14.0 ± 7.3†
	0.01 mM digoxin	18.8 ± 3.1*	11.0 ± 0.5*	1.83 ± 0.07*
	3 mM verapamil	27.0 ± 3.2*	10.3 ± 1.1*	1.68 ± 0.07*
Verapamil	Control	536 ± 6†	24.8 ± 1.4†	75.0 ± 5.8†
	1 mM vinblastine	362 ± 53*	13.4 ± 0.5*	74.0 ± 8.3
	3 mM verapamil	379 ± 18*	21.0 ± 2.4	75.5 ± 6.3

[^{3}H]Quinidine, [^{3}H]digoxin, and [^{3}H]verapamil with [^{14}C]*n*-butanol as the highly diffusible reference were injected into the carotid artery in the absence (control) or presence of inhibitors. Values represent means ± SE ($n = 3$–6 rats).

* $P < 0.05$, significantly different from each control.

† $P < 0.05$, significantly different from wild-type rats.

Discussion

Through comparison of wild-type and *mdr1a* knockout rats, our data directly indicated that P-gp works in the blood–ocular barriers as well as the BBB. Furthermore, our data strongly supported the suggestion of previous studies that the contribution of P-gp in the BRB is lower than that in the BBB.[16,17] It is suggested additionally that carrier-mediated influx transporters are present in the blood–ocular barriers and that there is a marked difference in the function of verapamil influx transporters between the retina and brain. Such influx transporters might be useful for systemic drug delivery to the retina without delivering drugs into the brain, avoiding potentially problematic central nervous system (CNS) side effects.

As shown in Figure 1, the trends in the RUI, AHUI, and BUI, obtained from the compounds undergoing passive diffusion in wild-type rats, corresponded with previous studies,[16,17] which indicated that with increasing lipophilicity, the RUI and BUI values increased but the AHUI values remained unchanged. Our results regarding the permeability of P-gp substrates across the BRB, BAB, and BBB in wild-type rats also were in agreement with these studies.[16,17] Therefore, the findings of all three studies using wild-type rats concur.[16,17]

P-gp is encoded by *mdr1a* and *mdr1b* isoforms in rat. Among quinidine, digoxin, and verapamil, the three P-gp substrates that we tested, there are no differences between *mdr1a* and *mdr1b* in P-gp substrate recognition.[18] However, *mdr1a* is expressed predominantly at the rat inner BRB[19] as well as the BBB,[20] compared to *mdr1b*. Additionally, our data showed that *mdr1a* mRNA was the predominant form at the outer BRB (Supplementary Fig. S1). These findings suggested that the *mdr1a* knockout rat is the optimal animal model for clarifying the function and impact of P-gp on blood–ocular barrier permeability, especially BRB permeability, compared to BBB permeability; nevertheless, it still is unclear which isoform is expressed predominantly in the rat BAB. Remarkably, the RUI values of [^{3}H]quinidine and [^{3}H]verapamil were greater than the predicted values from lipophilicity in wild-type rats, but were at the same level as predicted in *mdr1a* knockout rats (Fig. 1). This suggests that P-gp had little involvement in retinal uptake of quinidine and verapamil, and that influx transporters, rather than P-gp efflux, were the primary contributors.

Focusing on quinidine, the RUI and BUI of [^{3}H]quinidine in *mdr1a* knockout rats tended to decrease with 10 mM quinidine and significantly decreased with 3 mM verapamil (Fig. 3; Table 3), indicating that the impacts of influx transporters on BRB and BBB permeability to quinidine were at least 20%. Quinidine is a substrate of OCTN1[25] and OCTN2.[26] Recent studies have reported that OCTN1 and OCTN2 were expressed in the rat BRB[27] and BBB,[28] and also that quinidine drastically reduced the uptake of L-carnitine in immortalized rat retinal[27] and brain capillary endothelial cells.[28] Taken together with these previous findings, our results suggested that quinidine might be transported across the BRB and BBB via OCTN1 and/or OCTN2.

As shown in Figure 3 and Table 3, the RUI of [^{3}H]verapamil in *mdr1a* knockout rats significantly decreased with 1 mM vinblastine and 3 mM verapamil; in contrast, the BUI values were not influenced by such inhibitors. Therefore, the contribution of influx transporters to BRB permeability to verapamil was at least 30%. However, there was no impact on BBB influx. Regarding retinal influx transporters of verapamil, previous investigations suggest that the specificity of verapamil transport is very different from that of OCTN1 and OCTN2 using in vitro systems[24] and that novel organic cation transporters are involved in verapamil transport from the blood to the retina across the inner[24] and outer BRB.[29]

According to a previous report,[24] verapamil uptake by TR-iBRB cells (a conditionally immortalized rat retinal capillary endothelial cell line) was decreased with various cationic drugs with protective effects against retinal angiogenesis, such as propranolol, desipramine, nipradilol, brimonidine, and memantine, implying that these drugs for retinal diseases could be substrates of the novel influx transporters. In addition, our preliminary data showed that retinal [^{3}H]verapamil influx in *mdr1a* knockout rats was significantly reduced with 10 mM memantine, although the BUI was unchanged (data not shown). Taken together with these findings, the novel influx transporters recognizing verapamil on the BRB may be useful for systemic drug delivery to the retina without drugs permeating to the brain. Further studies are necessary to reveal the characteristics of these novel influx transporters.

To clarify the impact of P-gp on the retinal uptake of verapamil, integration plot analysis was performed and pharmacokinetic parameters were obtained by comparing *mdr1a* knockout rats to wild-type rats. $K_{in,retina}$ (0.824 mL/min·g retina) and $K_{in,brain}$ (0.140 mL/min·g brain) of [^{3}H]verapamil in wild-type rats (Table 2) corresponded with a previously published study.[24] $K_{in,aqueoushumor}$ and $K_{in,brain}$ in *mdr1a* knockout rats were greater than those in wild-type rats, although $K_{in,retina}$ was roughly equal, suggesting that the contribution of P-gp to BRB permeability is lower than that to BAB and BBB permeability. This result is consistent with the data obtained using uptake index methods. As shown in Figures 2A (retina) and 2C (brain), the apparent tissue–plasma concentration ratio, $C_{app}(t)/C_p(t)$ on the *y*-axis, reached a steady state over time, but its behavior in aqueous humor was different (Fig. 2B). One of the reasons for this difference might be the aqueous humor flow, whose turnover rate has been reported to be 2.23%/min in the rat.[30] However, it was less of an obstacle to compare the $K_{in,aqueoushumor}$ between wild-type and *mdr1a* knockout rats because aqueous humor flow was expected to be the same in both rat strains. In all tissues, the V_i values, which were comparable with the extracellular space (the intravascular volume and extracellular fluid) in the tissues, observed in *mdr1a* knockout rats were larger than those in wild-type rats. As no difference was observed between the intravascular volumes in wild-type and *mdr1a* knockout rats, which only differ in their lack of P-gp, this difference in V_i might be caused by extracellular fluid. To clarify the difference in V_i between wild-type and *mdr1a* knockout rats, it will be necessary to obtain experimental data within 30 seconds of intravenous injection in future experiments.

Statins, inhibitors of 3-hydroxy-3-methylglutaryl coenzyme A reductase, have neuroprotective effects in addition to cholesterol-lowering effects.[31,32] Orally administrated pitavastatin, a substrate of P-gp,[33] reduced *N*-methyl-D-aspartic acid–induced excitotoxic retinal cell death in rat.[34] Many statins have CNS side effects.[35] However, pitavastatin does not distribute to the rat brain,[36] suggesting that pitavastatin might undergo efflux from the brain via the P-gp of the BBB. As our data have shown, the impact of P-gp on BRB permeability to pitavastatin might be lower than that on BBB permeability. The difference in P-gp contribution might be exploitable when treating retinal disorders.

The present data revealed that [^{3}H]digoxin is transported to the retina and brain via carrier-mediated transporters (Fig. 3; Table 3). Previously, it has been suggested that digoxin is transported mainly to the brain via oatp1a4, which has an exceptionally high affinity for digoxin[37] and is localized on the abluminal and luminal membranes of the rat BBB.[38] Oatp1a4 is localized similarly on the abluminal and luminal domains of rat retinal capillary endothelial cells[39] and preferentially detected on the apical side of the rat RPE.[39,40] Our data indicated that the influx of [^{3}H]digoxin into retina and brain is decreased by 3 mM verapamil in *mdr1a* knockout rat, which is consistent with the previous report by Shitara et al.[41] who showed that verapamil inhibited the uptake of digoxin into oatp1a4-expressing LLC-PK$_1$ cells. According to Akanuma et al.,[39] oatp1c1 (oatp14; slco1c1) is expressed at both sides of the inner BRB and at the basolateral membrane of the RPE, but digoxin is not recognized by oatp1c1.[42] Oatp1a5, with a low affinity for digoxin,[43] also is expressed in rat retina[44,45] as mRNA, but it is not detected at the inner BRB.[19] In addition, digoxin overdose induces CNS symptoms, such as fatigue, anorexia, and vomiting, as well as visual symptoms, particularly halos around bright objects and changes in color perception.[46] Taken together with these previous findings, the influx transporter of digoxin into the retina is most likely to be oatp1a4. Further study is necessary to clarify the uptake mechanism of digoxin into the retina.

The BAB consists of two components, the nonpigmented ciliary epithelial cells and the iridial capillary endothelial cells, which are tightly joined and provide a controlled environment for internal ocular tissues. Previous in vitro studies have confirmed that P-gp is expressed in the iris, ciliary muscle, and ciliary nonpigmented cells.[10–12] In addition, the aqueous humor distribution of rhodamine 123 (as a substrate of P-gp) administered intravenously was markedly increased by topical administration of quinidine (as a P-gp inhibitor) in rabbits[47] and an increase in the aqueous humor concentration of quinidine (as a substrate of P-gp) following systemic administration was observed in the presence of verapamil (as a P-gp inhibitor).[48] Our comparison data clearly indicated that P-gp functions in the BAB as well as BRB and BBB, and also that the contribution of P-gp efflux of verapamil, measured in terms of the ratio of $K_{in,aqueoushumor}$ between wild-type and *mdr1a* knockout rats, is 66.1% (Table 2). Additionally, our results suggested that [^{3}H]quinidine, [^{3}H]digoxin, and [^{3}H]verapamil were permeated across the BAB by carrier-mediated influx transporters (Fig. 3; Table 3), since their uptake into the aqueous humor was decreased by P-gp inhibitors in *mdr1a* knockout rats. Oatp1a4 and oatp1b2 are expressed in the basolateral plasma membrane of the rat nonpigmented ciliary body epithelium and immunopositive protein bands for oatp1a5 are found in the rat ciliary body.[13] As mentioned before, oatp1a4 and oatp1a5, with high[37] and low[43] affinity for digoxin, respectively, might transport digoxin to the aqueous humor. To our knowledge, there are no reports on the expression of cation transporters in the BAB that recognize quinidine and/or verapamil as substrates. To elucidate the mechanism of quinidine and verapamil uptake into the aqueous humor, further study is needed.

Conclusions

To our knowledge, this is the first report, using *mdr1a* knockout rats, to reveal the impact of P-gp on drug permeability across the blood–ocular barriers and the presence of carrier-mediated influx transporters in the BRB and BAB. Our investigations clearly indicated the involvement of P-gp in the blood–ocular barriers and the BBB, as well as the lower impact of P-gp on BRB permeability to quinidine and verapamil than on BBB permeability. Furthermore, our inhibition studies suggested that carrier-mediated influx transporters are present in the blood–ocular barriers and that there is a marked difference in function of verapamil influx transporters between the retina and brain. Further studies are needed to understand the ocular distribution of drugs by characterizing their influx transport mechanisms across the BRB and BAB.

Acknowledgments

The authors thank Masakazu Yamamoto for contributing the quantitative RT-PCR values.

Disclosure: **S. Fujii**, Santen (E); **C. Setoguchi**, Santen (E); **K. Kawazu**, Santen (E); **K. Hosoya**, None

References

1. Kuno N, Fujii S. Dry age-related macular degeneration: recent progress of therapeutic approaches. *Curr Mol Pharmacol*. 2011;4:196–232.
2. Infeld DA, O'Shea JG. Diabetic retinopathy. *Postgrad Med J*. 1998;74:129–133.
3. van Soest S, Westerveld A, de Jong PT, Bleeker-Wagemakers EM, Bergen AA. Retinitis pigmentosa: defined from a molecular point of view. *Surv Ophthalmol*. 1999;43:321–334.
4. Kuno N, Fujii S. Recent advances in ocular drug delivery systems. *Polymers*. 2011;3:193–221.
5. Hosoya K, Tomi M. Advances in the cell biology of transport via the inner blood–retinal barrier: establishment of cell lines and transport functions. *Biol Pharm Bull*. 2005;28:1–8.
6. Cunha-Vaz J, Bernardes R, Lobo C. Blood–retinal barrier. *Eur J Ophthalmol*. 2011;21(suppl 6):S3–S9.
7. Hornof M, Toropainen E, Urtti A. Cell culture models of the ocular barriers. *Eur J Pharm Biopharm*. 2005;60:207–225.
8. Tomi M, Hosoya K. The role of blood–ocular barrier transporters in retinal drug disposition: an overview. *Expert Opin Drug Metab Toxicol*. 2010;6:1111–1124.
9. Tsuji A. Small molecular drug transfer across the blood–brain barrier via carrier-mediated transport systems. *NeuroRx*. 2005; 2:54–62.
10. Wu J, Zhang JJ, Koppel H, Jacob TJ. P-glycoprotein regulates a volume-activated chloride current in bovine non-pigmented ciliary epithelial cells. *J Physiol*. 1996;491(pt 3):743–755.
11. Schlingemann RO, Hofman P, Klooster J, Blaauwgeers HG, Van der Gaag R, Vrensen GF. Ciliary muscle capillaries have blood-tissue barrier characteristics. *Exp Eye Res*. 1998;66:747–754.
12. Zhang T, Xiang CD, Gale D, Carreiro S, Wu EY, Zhang EY. Drug transporter and cytochrome P450 mRNA expression in human ocular barriers: implications for ocular drug disposition. *Drug Metab Dispos*. 2008;36:1300–1307.
13. Gao B, Huber RD, Wenzel A, et al. Localization of organic anion transporting polypeptides in the rat and human ciliary body epithelium. *Exp Eye Res*. 2005;80:61–72.
14. Shen J, Cross ST, Tang-Liu DD, Welty DF. Evaluation of an immortalized retinal endothelial cell line as an in vitro model for drug transport studies across the blood–retinal barrier. *Pharm Res*. 2003;20:1357–1363.
15. Kennedy BG, Mangini NJ. P-glycoprotein expression in human retinal pigment epithelium. *Mol Vis*. 2002;8:422–430.
16. Toda R, Kawazu K, Oyabu M, Miyazaki T, Kiuchi Y. Comparison of drug permeabilities across the blood–retinal barrier, blood–aqueous humor barrier, and blood–brain barrier. *J Pharm Sci*. 2011;100:3904–3911.
17. Hosoya K, Yamamoto A, Akanuma S, Tachikawa M. Lipophilicity and transporter influence on blood-retinal barrier permeability: a comparison with blood–brain barrier permeability. *Pharm Res*. 2010;27:2715–2724.
18. Takeuchi T, Yoshitomi S, Higuchi T, et al. Establishment and characterization of the transformants stably-expressing MDR1 derived from various animal species in LLC-PK1. *Pharm Res*. 2006;23:1460–1472.
19. Tomi M, Hosoya K. Application of magnetically isolated rat retinal vascular endothelial cells for the determination of transporter gene expression levels at the inner blood–retinal barrier. *J Neurochem*. 2004;91:1244–1248.
20. Regina A, Koman A, Piciotti M, et al. Mrp1 multidrug resistance-associated protein and P-glycoprotein expression in rat brain microvessel endothelial cells. *J Neurochem*. 1998; 71:705–715.
21. Zamek-Gliszczynski MJ, Bedwell DW, Bao JQ, Higgins JW. Characterization of SAGE *Mdr1a* (P-gp), Bcrp, and Mrp2 knockout rats using loperamide, paclitaxel, sulfasalazine, and carboxydichlorofluorescein pharmacokinetics. *Drug Metab Dispos*. 2012;40:1825–1833.
22. Zamek-Gliszczynski MJ, Goldstein KM, Paulman A, Baker TK, Ryan TP. Minor compensatory changes in SAGE *Mdr1a* (P-gp), Bcrp, and Mrp2 knockout rats do not detract from their utility in the study of transporter-mediated pharmacokinetics. *Drug Metab Dispos*. 2013;41:1174–1178.
23. Alm A, Tornquist P. The uptake index method applied to studies on the blood–retinal barrier. I. A methodological study. *Acta Physiol Scand*. 1981;113:73–79.
24. Kubo Y, Kusagawa Y, Tachikawa M, Akanuma S, Hosoya K. Involvement of a novel organic cation transporter in verapamil transport across the inner blood–retinal barrier. *Pharm Res*. 2013;30:847–856.
25. Yabuuchi H, Tamai I, Nezu J, et al. Novel membrane transporter OCTN1 mediates multispecific, bidirectional, and pH-dependent transport of organic cations. *J Pharmacol Exp Ther*. 1999;289:768–773.
26. Ohashi R, Tamai I, Yabuuchi H, et al. Na(+)-dependent carnitine transport by organic cation transporter (OCTN2): its pharmacological and toxicological relevance. *J Pharmacol Exp Ther*. 1999;291:778–784.
27. Tachikawa M, Takeda Y, Tomi M, Hosoya K. Involvement of OCTN2 in the transport of acetyl-L-carnitine across the inner blood–retinal barrier. *Invest Ophthalmol Vis Sci*. 2010;51: 430–436.
28. Kido Y, Tamai I, Ohnari A, et al. Functional relevance of carnitine transporter OCTN2 to brain distribution of L-carnitine and acetyl-L-carnitine across the blood–brain barrier. *J Neurochem*. 2001;79:959–969.
29. Han YH, Sweet DH, Hu DN, Pritchard JB. Characterization of a novel cationic drug transporter in human retinal pigment epithelial cells. *J Pharmacol Exp Ther*. 2001;296:450–457.
30. Mermoud A, Baerveldt G, Minckler DS, Prata JA Jr, Rao NA. Aqueous humor dynamics in rats. *Graefes Arch Clin Exp Ophthalmol*. 1996;234(suppl 1):S198–S203.
31. Kawaji T, Inomata Y, Takano A, et al. Pitavastatin: protection against neuronal retinal damage induced by ischemia-reperfusion injury in rats. *Curr Eye Res*. 2007;32:991–997.
32. Honjo M, Tanihara H, Nishijima K, et al. Statin inhibits leukocyte-endothelial interaction and prevents neuronal death induced by ischemia-reperfusion injury in the rat retina. *Arch Ophthalmol*. 2002;120:1707–1713.
33. Shirasaka Y, Suzuki K, Nakanishi T, Tamai I. Differential effect of grapefruit juice on intestinal absorption of statins due to inhibition of organic anion transporting polypeptide and/or P-glycoprotein. *J Pharm Sci*. 2011;100:3843–3853.
34. Nakazawa T, Takahashi H, Nishijima K, et al. Pitavastatin prevents NMDA-induced retinal ganglion cell death by suppressing leukocyte recruitment. *J Neurochem*. 2007;100: 1018–1031.
35. Kikuchi R, Kusuhara H, Abe T, Endou H, Sugiyama Y. Involvement of multiple transporters in the efflux of 3-hydroxy-3-methylglutaryl-CoA reductase inhibitors across the blood–brain barrier. *J Pharmacol Exp Ther*. 2004;311:1147–1153.
36. Fujino H, Tsunenari Y, Koide T, Yonemitsu M, Yanagawa Y, Kimata H. Studies on the metabolic fate of NK-104, a new inhibitor of HMG-CoA reductase(2). *Drug Metab Pharmacokinet*. 1998;13:499–507.

Investigative Ophthalmology & Visual Science

37. Noe B, Hagenbuch B, Stieger B, Meier PJ. Isolation of a multispecific organic anion and cardiac glycoside transporter from rat brain. *Proc Natl Acad Sci U S A*. 1997;94:10346–10350.
38. Gao B, Stieger B, Noe B, Fritschy JM, Meier PJ. Localization of the organic anion transporting polypeptide 2 (Oatp2) in capillary endothelium and choroid plexus epithelium of rat brain. *J Histochem Cytochem*. 1999;47:1255–1263.
39. Akanuma SI, Hirose S, Tachikawa M, Hosoya KI. Localization of organic anion transporting polypeptide (Oatp) 1a4 and Oatp1c1 at the rat blood–retinal barrier. *Fluids Barriers CNS*. 2013;10:29.
40. Gao B, Wenzel A, Grimm C, et al. Localization of organic anion transport protein 2 in the apical region of rat retinal pigment epithelium. *Invest Ophthalmol Vis Sci*. 2002;43:510–514.
41. Shitara Y, Sugiyama D, Kusuhara H, et al. Comparative inhibitory effects of different compounds on rat oatpl (slc21a1)- and Oatp2 (Slc21a5)-mediated transport. *Pharm Res*. 2002;19:147–153.
42. Sugiyama D, Kusuhara H, Taniguchi H, et al. Functional characterization of rat brain-specific organic anion transporter (Oatp14) at the blood–brain barrier: high affinity transporter for thyroxine. *J Biol Chem*. 2003;278:43489–43495.
43. Cattori V, van Montfoort JE, Stieger B, et al. Localization of organic anion transporting polypeptide 4 (Oatp4) in rat liver and comparison of its substrate specificity with Oatp1, Oatp2 and Oatp3. *Pflugers Arch*. 2001;443:188–195.
44. Abe T. Molecular characterization and tissue distribution of a new organic anion transporter subtype (oatp3) that transports thyroid hormones and taurocholate and comparison with oatp2. *J Biol Chem*. 1998;273:22395–22401.
45. Walters HC, Craddock AL, Fusegawa H, Willingham MC, Dawson PA. Expression, transport properties, and chromosomal location of organic anion transporter subtype 3. *Am J Physiol Gastrointest Liver Physiol*. 2000;279:G1188–G1200.
46. Kelly RA, Smith TW. Recognition and management of digitalis toxicity. *Am J Cardiol*. 1992;69:108G–118G, discussion 118G–119G.
47. Kajikawa T, Mishima HK, Murakami T, Takano M. Role of P-glycoprotein in distribution of rhodamine 123 into aqueous humor in rabbits. *Curr Eye Res*. 1999;18:240–246.
48. Duvvuri S, Gandhi MD, Mitra AK. Effect of P-glycoprotein on the ocular disposition of a model substrate, quinidine. *Curr Eye Res*. 2003;27:345–353.

Investigative Ophthalmology & Visual Science